Journal of Engineering Physics and Thermophysics, Vol. 81, No. 4, 2008

HYDROGASDYNAMICS IN TECHNOLOGICAL PROCESSES

SIMULATION OF THE TURBULENT MIXING OF A PASSIVE IMPURITY IN A JET MIXER

A. D. Chornyi,[a] N. V. Kornev,[b] and E. Hassel[b]

UDC 532.517.4,532.526.5

Results of numerical simulation of the mixing of a turbulent jet with a cocurrent incompressible-fluid flow (Schmidt number Sc ≈ 1000) in a cylindrical channel of circular cross section (axisymmetric mixer) with the use of the standard k–ε turbulence model and different models for the averaged value of the mixture fraction and its variance have been given. For the problem of mixing of an inert passive impurity, two regimes of flow — the regime with the formation of a recirculation zone and that without its formation — have been considered. The formulated statistical model has been verified with the use of experimental data and results of calculation by large-eddy simulation.

Introduction. Jet flows belong to one of the most abundant types of shear flows met with in solving practical problems that are associated with the technologies used when devices for cleaning water media, burners, chemical reactors, heat exchangers, etc. are developed. The combinations of geometric parameters and mass flow rates used and the thermophysical properties of the transferred substances frequently make for turbulence in flows [1]. The problem of turbulent mixing of jets is of great interest. For example, in designing injection systems for feeding of liquid fuels, it is necessary to solve the problem of obtaining a uniform distribution of the transferred substances over the cross section of a mixing chamber which usually represents a cylindrically shaped channel where a jet develops in the cocurrent flow bounded by the walls. In this case we must study the behavior of wall flows, i.e., flows with mixing near solid walls, and to elucidate the influence of the walls on turbulent transfer in the channel. A fundamental understanding of such physical processes follows from an analysis of both experimental data and results obtained from mathematical models.

Models operating with differential equations for statistical moments of turbulence parameters with the use of different schemes of their closing remain the most viable for numerical realization in studying turbulent flows [2]. Unlike the methods of direct numerical simulation of turbulent flows [3] or simulation of large eddies [4], such an approach requires a smaller volume of computations and allows information on the averaged characteristics of jet flows at any point of the cylindrical channel as functions of the initial parameters of mixing flows.

In the present work, we give results of numerical simulation of the interaction of the turbulent axisymmetric jet with the cocurrent flow of an incompressible fluid (Schmidt number Sc ≈ 1000) in an axisymmetric mixer which represents a cylindrical channel with diameter D with a coaxially mounted internal tube with a diameter d. We have considered the problem of turbulent mixing of an inert passive impurity for different regimes of flow in such a mixer with verification of the standard k–ε turbulence model and different models of calculation of the averaged value of the mixture fraction and its variance by comparing the results obtained to experimental data [5] and to the results of large-eddy simulation [6].

[a]A. V. Luikov Heat and Mass Transfer Institute, National Academy of Sciences of Belarus, 15 P. Brovka Str., Minsk, 220072, Belarus; email: anchor@hmti.ac.by; [b]Fakultät für Mischinenbau und Schiffstechnik, Lehrstuhl für Technische Thermodynamik, Universität Rostok, 2 A. Einstein Str., Rostok, 18059, Germany. Translated from Inzhenerno-Fizicheskii Zhurnal, Vol. 81, No. 4, pp. 666–681, July–August, 2008. Original article submitted April 23, 2007.

In large-eddy simulation, anisotropic large-scale eddies with a scale exceeding the size of a finite-difference cell are faithfully reproduced by numerical integration of equations for realization of turbulent characteristics, whereas small-scale turbulent eddies are simulated with the use of either simple gradient relations or specially developed dynamic subgrid models [4]. Separation into large and small scales is carried out with a spatial filter where subgrid stresses and terms describing the influence of small scales on the transfer of the mixture components in the dynamic system must be parameterized with subgrid models. They have difficulties analogous to those existing when statistical models for the Reynolds-averaged quantities are closed. In this work, we use results obtained by large-eddy simulation with two subgrid models: the Smagorinskii model modified using the dynamic procedure of Germano and a mixed subgrid model constructed on similarity laws and with a stable procedure of calculation of the Smagorinskii constant [6].

Regimes of Turbulent Mixing in the Axisymmetric Jet Mixer. For the initial evaluation of the hydrodynamics and mixing of the turbulent axisymmetric jet of an incompressible fluid, blown out of the tube with a diameter d into the cylindrical channel with diameter D, the basic parameters are the ratio of the weight flow rates (ejection coefficient) $Q = Q_D/Q_d$, the geometric parameter $a = D/d$, and the ratio of the densities $b = \rho_d/\rho_D$ [1], and the Reynolds number Re_d composed from the parameters of the blown-out jet, the Prandtl number, and the Schmidt number. In the present work, the influence of the last two parameters is not investigated. At the same time, as follows from an analysis [7], the influence of the change in the Re_d value on the development of mixing is not so significant compared to the change in the ejection coefficient Q and the geometric parameter a.

It is quite sufficient to know these two parameters to determine, on the basis of the laws of conservation of mass and momentum, the ratio of the flow rates of the cocurrent flow U_D and the jet U_d at the mixer inlet $U_D/U_d = Qb/(a^2 - 1)$ and the parameters of the flow in the state of complete mixing — the ratio of the weight flow rates $Q_\infty/Q_d = Q + 1$, the average velocities $U_\infty/U_d = (1 + Qb)/a^2$, and the densities $\rho_\infty/\rho_d = (1 + Q)/(1 + Qb)$, and the pressure difference between the initial cross section and the mixer's cross section at which the state of the flow is homogeneous [1]:

$$\frac{\Delta p_\infty}{\rho_d U_d^2} = \frac{p_\infty - p_d}{\rho_d U_d^2} = \frac{a^2 - 1}{a^2}\left(1 - \frac{Q}{a^2 - 1}\right)\left(1 - \frac{Qb}{a^2 - 1}\right).$$

The values of Q_∞, U_∞, ρ_∞, and Δp_∞ are prescribed by the parameters of the flow under the assumption of complete mixing, i.e., on an infinite mixer length. However, the nonuniformity in the distributions of the hydro- and thermodynamic parameters of the flow is realized in different cross sections of the mixer of finite length. Therefore, using the ratios Q_∞/Q_d, U_∞/U_d, ρ_∞/ρ_d, and $\Delta p_\infty/(\rho_d U_d^2)$ we can evaluate the completeness of mixing in the mixer.

It is well known [8] that, in the axisymmetric mixer, there can be two topologically different regimes of flow: 1) a recirculation zone is formed at the channel walls; 2) this zone is not formed. Its occurrence can be explained using a simple model of trapping of a medium [8]. The jet flowing out of the internal tube injects part of the fluid from the cocurrent flow, which is in proportion to the difference of the velocities in the jet and in the flow. If the fluid volume injected by the jet per unit time is larger than the fluid flow rate in the cocurrent flow, the form of flow changes, the cocurrent flow separates from the mixer walls, and a recirculation zone occurs. Simple evaluations on the basis of this model lead to an inequality $1 + Q < D/d$ whose fulfillment means that flow in the mixer occurs with the formation of a recirculation zone (first regime). The results of experimental investigations confirm the validity of this rule (see, e.g., [5, 8–10]).

In [5], it has been shown that return flow at the walls of the cylindrical channel leads to a difference in the degeneration of turbulent characteristics, whereas the formation of the recirculation zone substantially influences the rate of mixing of the passive impurity transferred by the flow. For the ratios of the flow rates (Q = 1.3 and 5) and the diameters (D/d = 5), considered in [5], a homogeneous mixture in the first regime is formed 4 calibers earlier than it is formed in the second. For Q = 1.3, the recirculation zone begins with the distance $x/D > 0.1$; its center is between the cross sections $2.1 < x/D < 2.6$, and the boundary of its degeneration lies just behind the cross section x/D = 3.1. The influence of return flow on mixing can be analyzed by calculating the radius-averaged mixture fraction

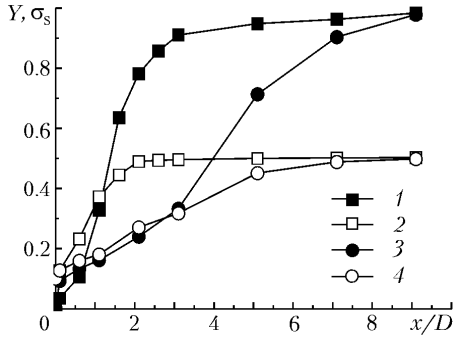

Fig. 1. Integral parameters Y (dark points) and σ_s (light points) for different mixing regimes: 1 and 2) Q = 1.3 and 3 and 4) 5.

$f_{av} = \left(\int_0^{1/2} r^2 \bar{f} dr\right) \Big/ \left(\int_0^{1/2} r^2 dr\right)$ (r is made dimensionless by means of D) [11]. It is precisely the rate of macromixing for both regimes of mixing that can initially be evaluated by the change in the normalized value $Y = (f_{av} - f_0)/(f_\infty - f_0)$ along the mixer (Fig. 1); here, the value of $f_0 = f_{av}$ in the initial cross section of the mixture is the same for both regimes, and $f_\infty = 1/(Q+1)$ is the f_{av} value in complete mixing. As is seen from the figure, mixing is carried out in such a manner only at a small distance ($x/D < 0.6$). Downstream macromixing is more rapid for the first regime and is close to its stage of completion beginning with x/D = 3.1 (Y approaches the asymptotic value Y = 1), whereas in the second regime, such a state is observed only at x/D = 9.1.

The quantity $\sigma_s = \sqrt{3\int_0^{1/2} r^2 \bar{f} dr \Big/ \int_0^{1/2} \bar{f} dr}$ (r and σ_s are made dimensionless by means of D) characterizes the transverse dimension of the jet and points to the probable position of the mixing layer formed at the boundary of interaction of the jet and the cocurrent flow in the case of the regime of mixing for Q = 5. For the regime of mixing for Q = 1.3, the integral parameter σ_s no longer carries information solely on the transverse dimension of the turbulent jet, since the interaction of the jet and the cocurrent flow is affected by the return flow at the mixer walls. This fact leads to a considerable content of the impurity over the entire cross section of the mixer. Such features of flow exert an influence on the change in the turbulent characteristics and must be allowed for when efficient statistical models are constructed.

Statistical Mixing Model on the Basis of the Reynolds Equations and Equations of the Mixture Fraction. Numerical simulation for different regimes of mixing has been carried out with allowance for the geometric and hydrodynamic properties of the axisymmetric jet mixer. We calculated the following Reynolds-averaged quantities: the longitudinal U and radial V components of the averaged velocity, the kinetic turbulence energy k and the rate of its dissipation ε, and the averaged value of the mixture fraction $\bar{f}$ and its variance σ^2.

In the axisymmetric formulation, for the functions sought, the differential conservation equations for the steady-state flow of an incompressible fluid with a constant density ρ have the general form [12]

$$\frac{\partial}{\partial x}(r\rho UF) + \frac{\partial}{\partial r}(r\rho VF) = \frac{\partial}{\partial x}\left(rD_{eff}\frac{\partial F}{\partial x}\right) + \frac{\partial}{\partial r}\left(rD_{eff}\frac{\partial F}{\partial r}\right) + rS\,. \tag{1}$$

Flow-Hydrodynamics Model. To calculate the longitudinal and radial components of the averaged velocity we use the continuity equation and the equations for each velocity component, which have the general form (1):

$$\frac{\partial (r\rho U)}{\partial x} + \frac{\partial (r\rho V)}{\partial r} = 0\,,$$

$$\frac{\partial}{\partial x}(\rho UV)+\frac{1}{r}\frac{\partial}{\partial r}(r\rho V^2)-\frac{\partial}{\partial x}\left(\mu_{\text{eff}}\frac{\partial V}{\partial x}\right)-\frac{1}{r}\frac{\partial}{\partial r}\left(r\mu_{\text{eff}}\frac{\partial V}{\partial r}\right)$$

$$=-\frac{\partial}{\partial r}\left(p+\frac{2}{3}\rho k\right)+\frac{\partial}{\partial x}\left(\mu_{\text{eff}}\frac{\partial U}{\partial r}\right)+\frac{1}{r}\frac{\partial}{\partial r}\left(r\mu_{\text{eff}}\frac{\partial V}{\partial r}\right)-\frac{2}{3}\frac{\mu_{\text{eff}}V}{r^2},$$

$$\frac{\partial}{\partial x}(\rho U^2)+\frac{1}{r}\frac{\partial}{\partial r}(r\rho VU)-\frac{\partial}{\partial x}\left(\mu_{\text{eff}}\frac{\partial U}{\partial x}\right)-\frac{1}{r}\frac{\partial}{\partial r}\left(r\mu_{\text{eff}}\frac{\partial U}{\partial r}\right)$$

$$=-\frac{\partial}{\partial x}\left(p+\frac{2}{3}\rho k\right)+\frac{\partial}{\partial x}\left(\mu_{\text{eff}}\frac{\partial U}{\partial x}\right)+\frac{1}{r}\frac{\partial}{\partial r}\left(r\mu_{\text{eff}}\frac{\partial V}{\partial x}\right),$$

where the effective viscosity μ_{eff} represents the sum of the molecular dynamic viscosity μ_{lam} and the turbulent viscosity μ_t.

Turbulence is characterized by two parameters: the kinetic turbulence energy k and the rate of its dissipation ε. Transfer equations for these functions are formulated with the use of the Boussinesq hypothesis and its analogs. This hypothesis underlies most of the engineering calculations of turbulent flows [2, 12]. An alternative to the Boussinesq hypothesis is separate simulation of all components of the turbulent-stress tensor, with the result that the corresponding transfer equation is constructed and solved for each Reynolds stress. Compared to the turbulent-viscosity-based models, such an approach possesses an important advantage in that it abandons the assumption of local isotropy, but it contains numerous empirical constants. Found for one type of flow, they do not necessarily guarantee improvement in the accuracy of calculation in another; a much larger volume of computations is required.

In the turbulent-viscosity-based models, unknown correlations are simulated by averaging the flow parameters in closing the equations for turbulent characteristics. The Boussinesq hypothesis enables us to write the Reynolds-stress tensor in terms of the strain-rate tensor of the averaged velocity with introduction of the notion of a turbulent viscosity μ_t by analogy with the molecular viscosity μ_{lam}. In this case for calculation of the turbulent characteristics we have obtained, from the Navier–Stokes equations, the standard k–ε model [2, 12]:

$$\frac{\partial}{\partial x}(\rho Uk)+\frac{1}{r}\frac{\partial}{\partial r}(r\rho Vk)-\frac{\partial}{\partial x}\left(\left(\mu_{\text{lam}}+\frac{\mu_t}{\sigma_k}\right)\frac{\partial k}{\partial x}\right)-\frac{1}{r}\frac{\partial}{\partial r}\left(r\left(\mu_{\text{lam}}+\frac{\mu_t}{\sigma_k}\right)\frac{\partial k}{\partial r}\right)=G-\rho\varepsilon,$$

$$\frac{\partial}{\partial x}(r\rho U\varepsilon)+\frac{1}{r}\frac{\partial}{\partial r}(\rho V\varepsilon)-\frac{\partial}{\partial x}\left(\left(\mu_{\text{lam}}+\frac{\mu_t}{\sigma_\varepsilon}\right)\frac{\partial \varepsilon}{\partial x}\right)-\frac{1}{r}\frac{\partial}{\partial r}\left(r\left(\mu_{\text{lam}}+\frac{\mu_t}{\sigma_\varepsilon}\right)\frac{\partial \varepsilon}{\partial r}\right)=C_{\varepsilon 1}\frac{\varepsilon}{k}G-C_{\varepsilon 2}\rho\frac{\varepsilon^2}{k}+\rho P_\varepsilon,$$

where

$$G=\mu_t\left(2\left(\left(\frac{\partial U}{\partial x}\right)^2+\left(\frac{\partial V}{\partial r}\right)^2+\left(\frac{V}{r}\right)^2\right)+\left(\frac{\partial U}{\partial r}+\frac{\partial V}{\partial x}\right)^2-\frac{2}{3}\frac{V}{r}\left(\frac{\partial U}{\partial x}+\frac{\partial V}{\partial r}\right)\right)-\frac{2}{3}\rho k\left(\frac{\partial U}{\partial x}+\frac{\partial V}{\partial r}\right);$$

$$P_\varepsilon=C_{\varepsilon 3}S_\varepsilon\varepsilon^2/k;\quad S_\varepsilon=\frac{1}{4}\frac{k}{\varepsilon}\left(\frac{\partial U}{\partial x}+\frac{\partial V}{\partial r}\right)\frac{V}{r}.$$

In the standard k–ε model, to determine the turbulent viscosity μ_t one uses the Kolmogorov–Prandtl formula $\mu_t = \rho C_\mu k^2/\varepsilon$ which is true for the assumption of developed locally isotropic turbulence, and the model's constants C_μ, σ_k, σ_ε, $C_{\varepsilon 1}$, $C_{\varepsilon 2}$, and $C_{\varepsilon 3}$ are prescribed from experiment [2, 12].

Following the recommendations of [12], standard values of the empirical constants C_μ, σ_k, σ_ε, $C_{\varepsilon 1}$, and $C_{\varepsilon 2}$ are used for the standard k–ε model in many engineering calculations of turbulent flows. They have been selected by comparing calculation results and experimental data for the wall jet and the mixing layer of an incompressible medium. However, it is well known [13, 14] that the standard k–ε turbulence model with this set of constants yields an overstated

result on the rate of spread and degeneration of axisymmetric free jets. Therefore, a modification of the equation for the dissipation rate ε by adding the extra term P_ε, which was constructed on the idea of stretching of eddies, was used to improve the accuracy of such a model, and the constant $C_{\varepsilon 3}$ was selected and was equal to 0.79 [13, 14]. It is noteworthy that such a model does not satisfy the realizability property [15] to which the turbulence model must correspond.

A different approach is related to the change in the constants $C_{\varepsilon 1}$ and $C_{\varepsilon 2}$ in terms of the equation that are responsible for the enhancement and attenuation of the kinetic-energy dissipation [13, 16–20]. It is well known [21] that the rate of spread of a circular jet decreases with increase in the $C_{\varepsilon 1}/C_{\varepsilon 2}$ ratio. Increase only in the constant $C_{\varepsilon 1}$ also leads to a lag of the degeneration of the jet occupying a stretched and simultaneously contracted flow region in this case. The modification of [13, 16] uses the fixed value $C_{\varepsilon 1} = 1.6$. In [22], selection of C_μ and $C_{\varepsilon 2}$ is dependent on the rate of degeneration of the velocity and on the radius of opening of the jet [17]:

$$C_\mu = 0.09 - 0.04\xi\,; \quad C_{\varepsilon 2} = 1.92 - 0.0667\xi\,; \quad \xi = \left| \frac{r_d}{2\,(U_{\text{ax}} - U_D)} \left(\frac{\partial U_{\text{ax}}}{\partial x} - \left| \frac{\partial U_{\text{ax}}}{\partial x} \right| \right) \right|^{0.2}.$$

The assumption of the linear dependence of r_d on x and the inverse dependence of U_{ax} on the longitudinal coordinate [1] makes it possible to evaluate the constants as $C_\mu = 0.06$ and $C_{\varepsilon 2} = 1.87$ [22].

Mixing Model. The parameter characterizing the rate of turbulent mixing was the mixture fraction f which was determined as the ratio of the local concentration of a dissolved passive impurity C to its concentration C_0 at the exit of the jet in the initial cross section of the mixer. Then we had $f = 1$ at exit of the jet and $f = 0$ at entry of the cocurrent flow.

An analysis was made from the change in the first two statistical moments of the mixture fraction: the average value $\bar{f}$ and the variance of pulsations σ^2. The averaged value $\bar{f}$ is the characteristic of large-scale transfer of substances dissolved in the medium, i.e., the rate of attainment of macromixing. Mixing to the molecular scale (small-scale mixing, i.e., micromixing) is determined by the degeneration of pulsations in the concentration distribution of the transferred substances in the flow region and is related to the change in the variance of the mixture fraction σ^2 due to the scalar dissipation with a rate ε_s. The equations of the $\bar{f}$–σ^2 mixing model [12] that are written with the use of the gradient hypothesis for turbulent scalar flows are identical to the transfer equations (1):

$$\frac{\partial}{\partial x}(\rho U\bar{f}) + \frac{1}{r}\frac{\partial}{\partial r}(r\rho V\bar{f}) - \frac{\partial}{\partial x}\left(\rho\,(D_{\text{lam}} + D_{\text{t}})\frac{\partial \bar{f}}{\partial x}\right) - \frac{1}{r}\frac{\partial}{\partial r}\left(r\rho\,(D_{\text{lam}} + D_{\text{t}})\frac{\partial \bar{f}}{\partial r}\right) = 0\,,$$

$$\frac{\partial}{\partial x}(\rho U\sigma^2) + \frac{1}{r}\frac{\partial}{\partial r}(r\rho V\sigma^2) - \frac{\partial}{\partial x}\left(\rho\,(D_{\text{lam}} + D_{\text{t}})\frac{\partial \sigma^2}{\partial x}\right) - \frac{1}{r}\frac{\partial}{\partial r}\left(r\rho\,(D_{\text{lam}} + D_{\text{t}})\frac{\partial \sigma^2}{\partial r}\right)$$

$$= C_{\sigma 1}\frac{\mu_{\text{t}}}{\text{Sc}_{\text{t}}}\left(\left(\frac{\partial \bar{f}}{\partial x}\right)^2 + \left(\frac{\partial \bar{f}}{\partial r}\right)^2\right) - \rho\varepsilon_{\text{s}}\,,$$

where $C_{\sigma 1} = 2$ and $\rho(D_{\text{lam}} + D_{\text{t}}) = \mu_{\text{lam}}/\text{Sc} + \mu_{\text{t}}/\text{Sc}_{\text{t}}$. The value of $\text{Sc}_{\text{t}} = \mu_{\text{t}}/(\rho D_{\text{t}})$ is usually taken to be equal to 0.7.

For the equation of the variance σ^2, we must prescribe the method of determining the scalar-dissipation rate ε_s. One model used for ε_s is the algebraic model based on the assumption of the change in the ratio of the time scales of the turbulent velocity fields $\tau_{\text{t}} = k/\varepsilon$ and the scalar $\tau_{\text{s}} = \sigma^2/\varepsilon_{\text{s}}$ (scalar-mixing time) $R = \tau_{\text{t}}/\tau_{\text{s}}$ [12]. In this case we have $\varepsilon_{\text{s}} = \sigma^2/\tau_{\text{s}} = R\sigma^2/\tau_{\text{t}}$. The assumption of constancy of R (usually $R = 2$) enables us to write a widely used mixing model. It holds true for the fully developed scalar spectrum, i.e., mixing is assumed to occur on all length and true scales. Furthermore, dissipation must be in equilibrium with the production of pulsations of the mixture fraction on large scales, whereas the production of velocity and scalar pulsations must occur similarly and be dependent on the same physical mechanisms.

The model at $R = 2$ is used predominantly in investigations of gas flows with molecular Schmidt numbers Sc of the order of unity. Modification of the algebraic expression for the characteristic time scale of scalar dissipation $\tau_{\text{s}} =$

$\frac{2}{2+\mathrm{Sc}^{-1}}\left(\frac{3}{2}\tau_t+\frac{1}{2}\ln(\mathrm{Sc})\tau_K\right)$ has been proposed for determination of the influence of the Sc value on the change in the turbulent characteristics [23]. In this case the ratio of the characteristic time scale $R = \left(2+\mathrm{Sc}^{-1}\right)/\left(3+\mathrm{Re}_t^{-1}\ln \mathrm{Sc}\right)$, with account for the known expression $\tau_K/\tau_t = 1/\sqrt{\mathrm{Re}_t}$, is a variable and is dependent on both the Schmidt number Sc and the turbulent Reynolds number Re_t which is calculated from the standard velocity pulsation $u' = \sqrt{2k/3}$ and the length scale of turbulence l_t. When $\mathrm{Sc} \to 1$, the last model degenerates to the model for $R = 1$.

The model constructed with allowance for the features of the mixing of media with large Schmidt numbers Sc is the cascade (multiscale) $\bar{f}$–σ^2 model [23]. In this case the dissipation and the production of mixture-fraction pulsations are determined by their change in three stages characterized by the inertial-convective, viscoconvective, and viscodiffusion ranges of the energy scalar spectrum [23, 24]. The intrinsic component of the variance $\left(\sigma_1^2, \sigma_2^2, \sigma_3^3\right)$ with its own transfer equations of the form (1) [23]

$$\frac{\partial}{\partial x}(\rho U\sigma_1^2)+\frac{1}{r}\frac{\partial}{\partial r}(r\rho V\sigma_1^2)-\frac{\partial}{\partial x}\left(\rho\,(D_{\mathrm{lam}}+D_t)\frac{\partial\sigma_1^2}{\partial x}\right)-\frac{1}{r}\frac{\partial}{\partial r}\left(r\rho\,(D_{\mathrm{lam}}+D_t)\frac{\partial\sigma_1^2}{\partial r}\right)$$

$$=C_{\sigma1}\frac{\mu_t}{\mathrm{Sc}_t}\left(\left(\frac{\partial\bar{f}}{\partial x}\right)^2+\left(\frac{\partial\bar{f}}{\partial r}\right)^2\right)-\rho C_{\sigma2}\frac{\varepsilon}{k}\sigma_1^2,$$

$$\frac{\partial}{\partial x}(\rho U\sigma_2^2)+\frac{1}{r}\frac{\partial}{\partial r}(r\rho V\sigma_2^2)-\frac{\partial}{\partial x}\left(\rho\,(D_{\mathrm{lam}}+D_t)\frac{\partial\sigma_2^2}{\partial x}\right)-\frac{1}{r}\frac{\partial}{\partial r}\left(r\rho\,(D_{\mathrm{lam}}+D_t)\frac{\partial\sigma_2^2}{\partial r}\right)$$

$$=\rho C_{\sigma2}\frac{\varepsilon}{k}\sigma_1^2-\rho E\sigma_2^2,$$

$$\frac{\partial}{\partial x}(\rho U\sigma_3^2)+\frac{1}{r}\frac{\partial}{\partial r}(r\rho V\sigma_3^2)-\frac{\partial}{\partial x}\left(\rho\,(D_{\mathrm{lam}}+D_t)\frac{\partial\sigma_3^2}{\partial x}\right)-\frac{1}{r}\frac{\partial}{\partial r}\left(r\rho\,(D_{\mathrm{lam}}+D_t)\frac{\partial\sigma_3^2}{\partial r}\right)$$

$$=\rho E\sigma_2^2-\rho G\sigma_3^2,$$

for which $C_{\sigma1} = 2$, $C_{\sigma2} = 2$, $\mathrm{Sc}_t = 0.7$, $E = 0.058\tau_K^{-1/2}$, and $G = (0.330 + 17{,}050/\mathrm{Sc})E$, is responsible for each stage. The equation for the total dispersion $\sigma^2 = \sigma_1^2+\sigma_2^2+\sigma_3^3$

$$\frac{\partial}{\partial x}(\rho U\sigma^2)+\frac{1}{r}\frac{\partial}{\partial r}(r\rho V\sigma^2)-\frac{\partial}{\partial x}\left(\rho\,(D_{\mathrm{lam}}+D_t)\frac{\partial\sigma^2}{\partial x}\right)-\frac{1}{r}\frac{\partial}{\partial r}\left(r\rho\,(D_{\mathrm{lam}}+D_t)\frac{\partial\sigma^2}{\partial r}\right)$$

$$=C_{\sigma1}\frac{\mu_t}{\mathrm{Sc}_t}\left(\left(\frac{\partial\bar{f}}{\partial x}\right)^2+\left(\frac{\partial\bar{f}}{\partial r}\right)^2\right)-\rho G\sigma_3^2$$

yields that in the cascade model [23], pulsations are produced by large-scale transfer and dissipate in the viscodiffusion range with a viscodiffusion-mixing rate determined by the frequency characteristic $G = (0.330 + 17{,}050/\mathrm{Sc})E$; the parameter $E = 0.058\tau_K^{-1/2}$ is responsible for micromixing in small dissipative eddies [23, 24].

Realization of the Statistical Model and Boundary Conditions. Because of the symmetry of the mixer structure, we considered, in the calculation, a two-dimensional rectangular 0.6×0.025 m region in the longitudinal direction from the outlet plane of the internal tube and in the radial direction from the mixer axis. The calculations were carried out on a nonuniform spatial grid with the clustering of nodes at the outlet plane of the internal tube, at the flow axis, and in the wall region. The number of cells was 60 in the radial direction and 880 in the longitudinal direction. The transfer equations for the functions sought were solved with the use of the FLUENT commercial package

TABLE 1. Parameters of the Mixing Regimes

Regime No.	Q	a	b	$\mathrm{Re}_D/\mathrm{Re}_d$	U_D/U_d	U_∞/U_d	f_∞
1	1.3	5	1	0.27	0.054	0.092	0.43
2	5	5	1	1.042	0.2083	0.24	0.17

with a discretization scheme of second order and a refinement of pressure by the Patankar–Spalding SIMPLE algorithm [12]. The iterations ended upon attaining an accuracy of the order of 10^{-6} for all functions. The UDS module with the software procedures written in the macroses language of the FLUENT package was used for realization of the f–σ^2 cascade model.

We determined the initial profiles for all the functions sought in the initial cross section of the computational domain (exit plane of the jet). It is well known that the longitudinal-velocity profile is described by the parabolic law $U = U_{\max}(1 - (2r/d)^2)$ for laminar flow in a tube with a diameter d, and the radial velocity is $V = 0$. At the same time, the power law $U = U_{\max}\left(1 - \dfrac{2r}{d}\right)^{1/n}$ and $V = 0$ hold true for the developed turbulent flow in the tube. In [1], the value of n is equal to 7. An alternative method of prescribing the initial profiles is their evaluation from the available experimental distributions. In the present investigation, simulation was carried out when both a power-law profile and a constant longitudinal velocity were prescribed at exit of the jet. The profiles of the longitudinal velocity U at the outlet of the internal tube and the inlet of the mixer were evaluated from the available experimental data [5]. The profile of the longitudinal velocity U, measured near the internal-tube outlet, was quite well approximated by the power law for $n = 10$ with the velocity $U_{\max}$ equal to the velocity U_d. A longitudinal-velocity profile consistent with experimental data [5] was established at entry of the cocurrent flow. The transverse velocity component was equal to zero.

The profiles of turbulent characteristics of the jet and the cocurrent flow were determined from the relations for the kinetic energy $k = 1.5\mathrm{Tu}^2U^2$ and the rate of its dissipation $\varepsilon = C_\mu^3 k^{3/2}/l_t$. The turbulence intensity $\mathrm{Tu} = u'/U$ was evaluated as $\mathrm{Tu} = 0.16\mathrm{Re}_h^{-1/8}$. The initial length scale of turbulence l_t was prescribed by the relation $l_t = 0.07D_h$. The Reynolds number Re_h was calculated from the hydraulic parameter D_h determined in terms of the open area of the flow and the wetted perimeter of the domain for which the boundary condition was specified. We had $D_h = d$ for the exit of the jet and $D_h = D - d$ for the entry of the cocurrent flow. According to definition, the averaged value of the mixture fraction f was equal to unity at exit of the jet and took the zero value at entry of the cocurrent flow; the values of the variance σ^2 and its components σ_i^2 (i = 1, 2, and 3) were equal to zero.

The condition of equality to zero of the radial component of the averaged velocity V and the derivatives $\partial(\rho F)/\partial r$, where $F = U$, k, ε, f, or σ^2 and σ_i^2, was set on the symmetry axis. At the outlet boundary of the computational domain, we had $\partial(\rho V)/\partial r = 0$ for all functions. In this case the continuity equation degenerated to $\partial(\rho F)/\partial x = 0$, whence it followed that the radial velocity was $V = 0$ at the entire outlet boundary because of its equality to zero on the symmetry axis.

The adhesion condition for the components of the velocity U and V and the equality to zero of the derivatives $\partial(\rho F)/\partial r$, where $F = f$, σ^2, and σ_i^2, were set on the walls. The equations for the k–ε model hold true for developed locally isotropic turbulence. Near the wall, there is a boundary layer in which this assumption is violated, i.e., the turbulent Reynolds number is $\mathrm{Re}_t << 1$. Therefore, the method of wall functions with the logarithmic wall law was used near the wall to prescribe the turbulent characteristics (kinetic turbulence energy k and the rate of its dissipation ε) [12].

Below, we consider the turbulent transfer of a passive impurity (rhodamine) contained in the jet and its mixing with the medium of the cocurrent flow for two regimes of mixing: with a recirculation zone (1) and without it (2) (Table 1). Numerical simulation is carried out with allowance for the geometric and hydrodynamic properties of an axisymmetric jet mixer which was used in the experimental investigation of [5] (ρ = 1000 kg/m^3, d = 0.01 m, U_d = 1 m/sec, Schmidt number Sc = 100, and Reynolds number $\mathrm{Re}_d = \rho U_d/\mu_{\mathrm{lam}}$ = 10,000).

Change in the Averaged Velocity and Its Standard Pulsations. The behavior of U_{ax} (Fig. 2a and b) demonstrates that the degeneration of the averaged velocity for both mixing regimes is the same to the distance $x/D < 1.1$. In the initial cross section (near the exit of the jet), the injected jet is close to developed turbulent flow in character. The length of the potential core in which the jet is weakly dependent on viscosity and which is observed in jet flows

TABLE 2. Constants of the Standard k–ε Turbulence Model

Model No.	Literature source	C_μ	σ_k	σ_ε	$C_{\varepsilon 1}$	$C_{\varepsilon 2}$	$C_{\varepsilon 1}/C_{\varepsilon 2}$	$C_{\varepsilon 3}$
1	[11]	0.09	1	1.3	1.44	1.92	0.75	0
2	[15]	0.09	1	1.3	1.44	1.92	0.75	0.79
3	[21]	0.09	1	1.3	1.44	1.80	0.80	0
4	[14]	0.09	1	1.3	1.60	1.92	0.83	0
5	[21]	0.09	1	1.3	1.44	1.87	0.77	0

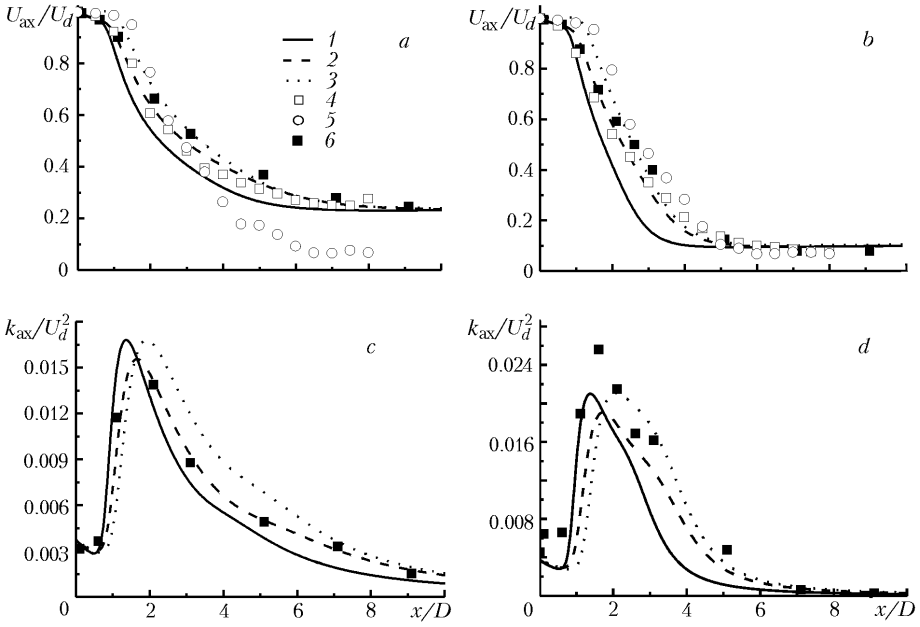

Fig. 2. Longitudinal component of the averaged velocity (a and b) and the kinetic turbulence energy (c and d) along the mixer axis for two mixing regimes (a and c) Q = 5 and b and d) 1.3), obtained according to different computational approaches: the standard k–ε model — model 1 (Table 2) (1); model 5 (Table 2) with a power-law velocity profile at exit of the jet (2) and model 5 (Table 2) without this profile (3); large-eddy simulation with a subgrid mixed model (4) [6] and with a subgrid Smagorinskii model with allowance for the Germano procedure (5) [6]; 6) experimental data of [5].

[1] is quite short. Just behind the cross section x/D = 1.1, the velocity U_{ax} on the mixer axis degenerates much more rapidly for Q = 1.3 than for Q = 5 and attains its asymptotic value U_∞ by the cross section x/D = 6. The kinetic turbulence energy grows from the initial cross section downstream and attains its maximum in the cross section x/D = 2.1, after which it rapidly degenerates with a certain leading rate for Q = 1.3. This leads to the fact that the kinetic energy behind the rear boundary of the recirculation zone ($x/D > 3.1$) is twice as low as that for Q = 5 and nearly completely degenerates after the cross section x/D = 6. This fact demonstrates that the complete mixing takes shorter time in the case of formation of a recirculation zone in the jet mixer.

In [25], a number of the sets of constants (Table 2) used in investigating free turbulent jets are used with the aim to verify the standard k–ε turbulence model for a circular turbulent jet in its mixing with a cocurrent flow bounded by the walls of a cylindrical channel. The numerical simulation carried out in [25] with different sets of model constant shows that the modifications correspond to a variable degree to experimental data [5] for both the velocity U_{ax} and the kinetic turbulence energy k compared to the standard set (model 1, Table 2). The use of the extra term P_ε in the equation for dissipation (model 2, Table 2) is absolutely insufficient for agreement. At the same time, increase in the $C_{\varepsilon 1}/C_{\varepsilon 2}$ ratio (models 3–5, Table 2) points to the much slower rate of opening and degeneration of the

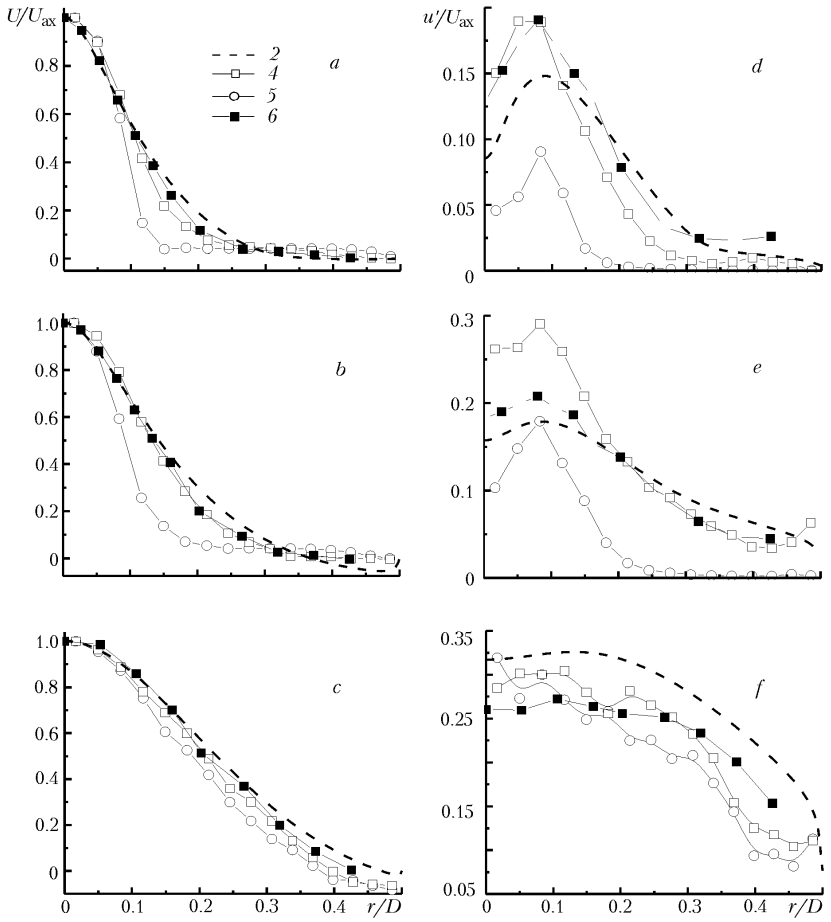

Fig. 3. Longitudinal component of the averaged velocity (a–c) and its standard pulsation (d–f) for Q = 1.3 in the mixer's cross section at different distances from the exit of the jet: a and d) x/D = 1.1, b and e) 1.6, and c and f) 3.1. Notation 2, 4, 5, and 6 is the same as in Fig. 2.

circular jet than that recorded by models 1 and 2. The best agreement with experiment [5] for the velocity U_{ax} is demonstrated by model 4 for both mixing regimes; however, the level of kinetic energy from calculation is understated. Models 3 and 5 yield the identical (close to that experimental) result on degeneration of the velocity U_{ax} along the mixer axis (Fig. 2a and b). It is noteworthy that model 5 is the best one from those considered from the viewpoint of the accuracy of prediction of the kinetic energy k for both mixing regimes (Fig. 2c and d); for Q = 5, the agreement of the change in this characteristic of turbulence with experimental data [5] is fairly complete (Fig. 2c).

The use of a constant value of the longitudinal velocity U instead of the profile in the form of a power law as the boundary condition at exit of the jet for calculation gives rise to the region with a constant velocity to the distance x/D = 1.5 for both mixing regimes (Fig. 2a and b). This is in disagreement with the change, in the initial region, in the longitudinal velocity obtained both experimentally and by large-eddy simulation with the use of a subgrid mixed model and a stable procedure of calculation of the Smagorinskii constant [6] and from the standard k–ε model (model 5, Table 2) with the power-law velocity profile being prescribed. Furthermore, the assumption that the velocity at exit of the jet is constant leads to a lag of the degeneration of the calculated kinetic turbulence energy compared to that obtained experimentally (Fig. 2c and d).

Figures 3 and 4 demonstrate the change in the longitudinal component of the averaged velocity U and the standard pulsations $u' = \sqrt{2k/3}$ in the mixer's cross section at different distances from the cross section of blowing-out of the turbulent jet in different mixing regimes.

When Q = 1.3, return flow exists in a thin layer near the mixer wall, which is reflected in the change of sign of the averaged velocity in the cross sections x/D = 1.6 and 3.1 (Fig. 3b and c). The level of turbulent pulsations

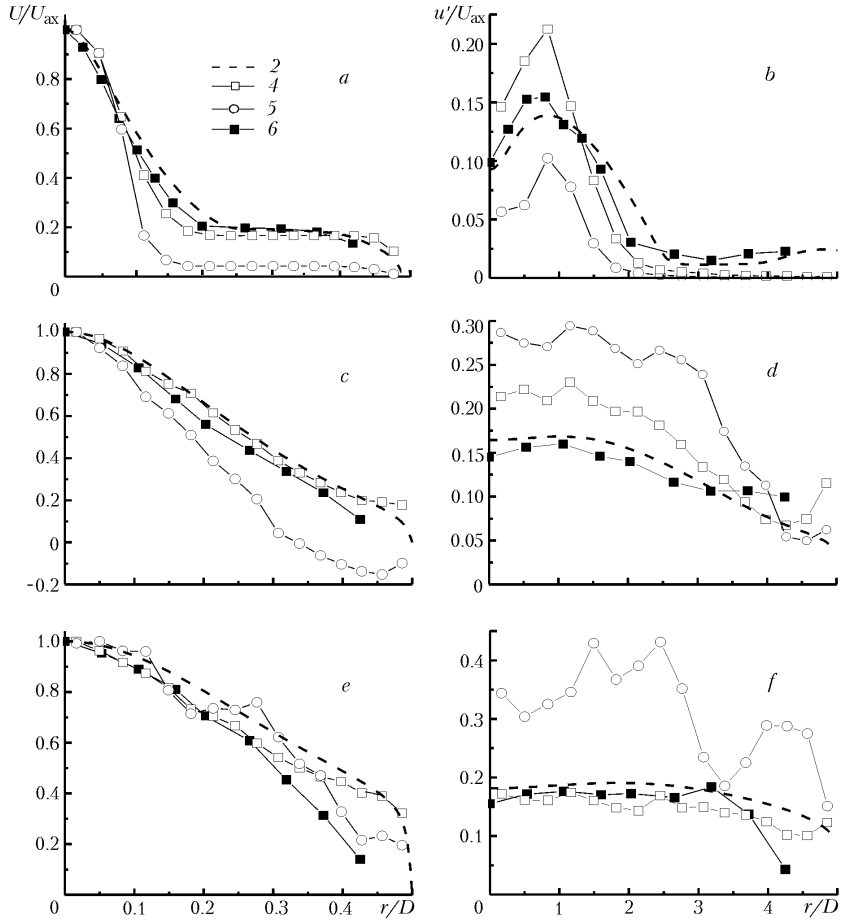

Fig. 4. Longitudinal component of the averaged velocity (a–c) and its standard pulsation (d–f) for Q = 5 in the mixer's cross section at different distances from the exit of the jet: a and d) x/D = 1.1, b and e) 3.1, c and f) 3.1. Notation 2, 4, 5, and 6 is the same as in Fig. 2.

grows over the mixer's cross section downstream (Fig. 3d–f), pointing to the development of a recirculation zone. However, as has been shown in [5, 26], the maximum turbulent velocity pulsations are recorded immediately behind the recirculation zone, not in it, in the cross section x/D = 5.1. In turn the formation of a uniform distribution of the averaged velocity for $x/D > 5.1$ is responsible for the decrease in pulsations [5, 26].

An analysis made in [5, 26] has shown that the regime of mixing without a recirculation zone for Q = 5 is characterized by the higher velocity of the cocurrent flow and the monotonic expansion of the velocity profile reflecting the development of jet flow (Fig. 4). When $x/D < 2.1$ the profiles of turbulent pulsations are much narrower, and their maximum values are lower than those in the mixing regime considered above. Despite the by no means uniform distribution of the averaged velocity over the mixer's cross section in the investigated range of distances $x/D < 9.1$, the profiles of turbulent pulsations in the cross sections x/D = 7.1 and 9.1 are quite uniform. Their values are appreciably lower than those existing in analogous cross sections in the mixing regime with a recirculation zone, where the averaged-velocity distribution is more uniform.

This dynamics of interaction of the turbulent jet and the cocurrent flow in the axisymmetric mixer for both mixing regimes is in fairly good agreement with the results of calculation by large-eddy simulation with the use of a subgrid mixed model with a stable procedure of calculation of the Smagorinskii constant [6] and the standard k–ε model (model 5, Table 2) with the power-law velocity profile being prescribed (Figs. 3 and 4).

Change in the Averaged Value of the Mixture Fraction and in Its Variance. Figure 5a and b compares results of the change in the averaged value of the mixture fraction $f_{ax} = \bar{f}(x, 0)$ along the mixer axis for both mixing regimes (the results have been obtained using different turbulence models) and experiment [5].

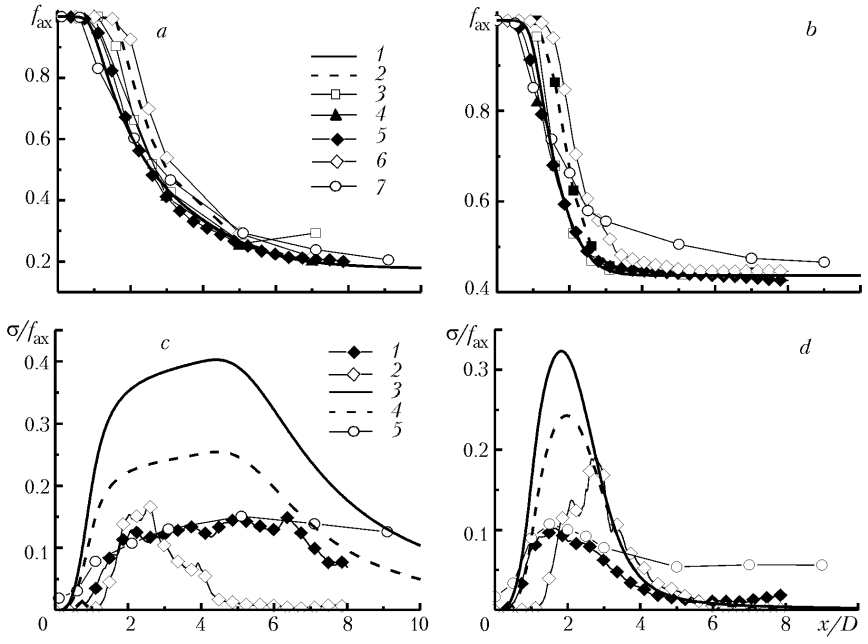

Fig. 5. Averaged mixture fraction $\bar{f}$ (1) standard k–ε model (model 5, Table 2); 2) k–ε model [6]; 3) k–ω model [6]; 4) model for Reynolds stresses [6]; 5) large-eddy simulation with a subgrid mixed model and 6) with a subgrid Smagorinskii model with allowance for the Germano procedure [6]; 7) experimental data of [5] and the variance σ (1) large-eddy simulation with a subgrid mixed model [6]; 2) with a subgrid Smagorinskii model with allowance for the Germano dynamic procedure [6]; 3) cascade model [22]; 4) mixing model for R = 2; 5) experimental data of [5]) along the mixer axis for Q = 5 (a and c) and 1.3 (b and d).

As is seen, near the exit of the turbulent jet, there is a region with a constant concentration of the impurity up to x/D = 1 for both mixing regimes (Fig. 5a and b). However, the results obtained using different statistical turbulence models [6] and large-eddy simulation with a subgrid Smagorinskii model with allowance for the dynamic procedure of Germano [6] overstate the length of this region by twofold. Next we have the process of intense mixing to form a uniform concentration distribution, which is reflected in the fact that f_{ax} attains its asymptotic value f_∞ (regime of complete mixing) in calculations by all the models. For Q = 1.3 (Fig. 5b), such attainment for all the models occurs with a certain leading rate compared to experimental data and approximately 4 calibers earlier than for Q = 5 (Fig. 5a).

Calculation of f_{ax} along the mixer axis with the use of the standard k–ε model (model 5, Table 2) and with the velocity profile in the form of a power law at exit of the turbulent jet gives a result analogous to calculations by the statistical model for Reynolds stresses and by large-eddy simulation with the use of a subgrid mixed model with a stable procedure of calculation of the Smagorinskii constant [6] for both mixing regimes (Fig. 5a and b).

Figure 5c and d gives the change in the relative variance σ/f_{ax} of the mixture fraction. Numerical results obtained with the use of the mixing model for a constant ratio R = 2 and the cascade model [23] are compared to experimental data [5] and calculation [6] by large-eddy simulation with two subgrid models: the mixed model and the Smagorinskii model with a dynamic Germano procedure [6].

For the above mixing regimes, both models give a result overstated relative to experiment and large-eddy simulation in the change in σ along the mixer axis (Fig. 5c and d). However, the general trend holds: first we have an increase in the level of relative pulsations because of the dynamic mixing of the jet and the medium entrapped from the cocurrent flow due to the large-scale convective transfer and turbulent diffusion (macromixing) and thereafter the degeneration of pulsations due to the intense dissipative process. The maximum level of pulsations in the cascade model [23] is nearly 1.5 times higher than the level obtained for the mixing model at R = 2 and nearly thrice as high

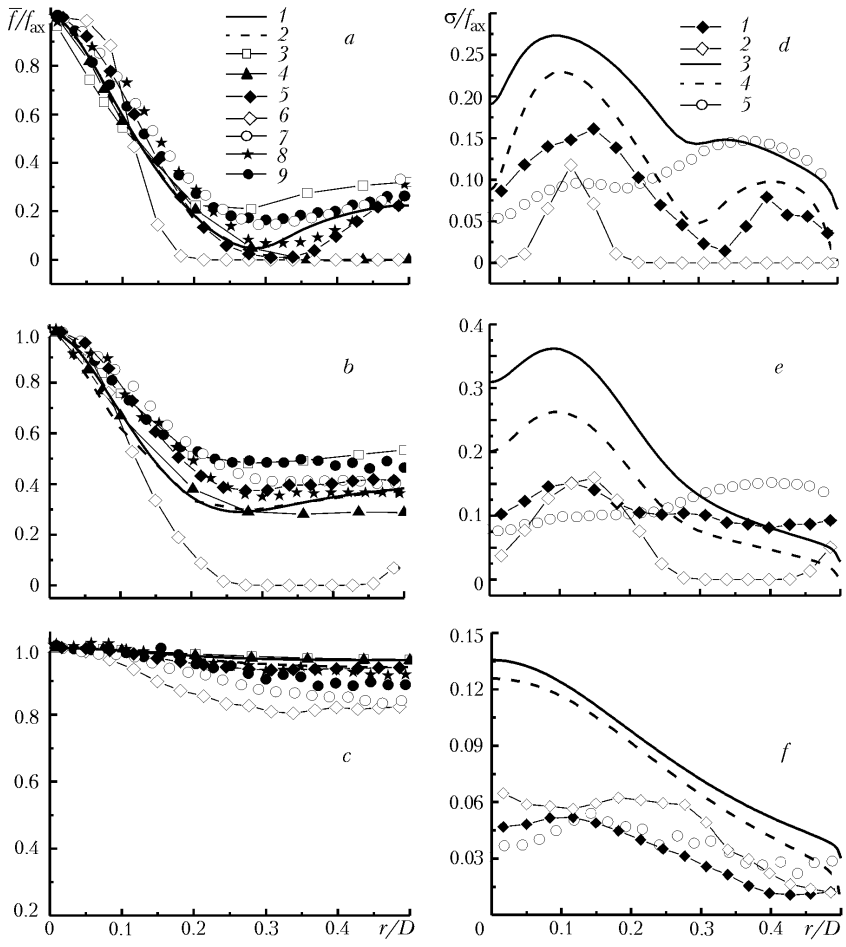

Fig. 6. Averaged mixture fraction $\bar{f}$ (a–c) and its variance σ (d–f) for Q = 1.3 in the mixer's cross section at different distances from the exit of the jet: a and d) x/D = 1.1, b and e) 1.6, and c and f) 3.1 (experimental data of [5]: 7) α = 90°, 8) 0°, 9) 180°; calculation results, curves). Notation is the same as in Fig. 5.

as the experimental level. An analogous result has been given in [24], where the results of the cascade model are compared to experiment [27].

The obtained f distribution in the flow demonstrates the qualitative difference in the structure of impurity transfer for both mixing regimes because of the existence of the recirculation zone with a position consistent with experimental data [5] near the mixer walls for Q = 1.3. Such a fact is reflected in the shape of the $f(x, r)$ profile in the mixer's cross section (Fig. 6a and b). The transfer, by return flow, of the passive impurity along the mixer walls in the direction opposite to the jet motion increases its concentration in this region, which causes f to grow. The f profile expands downstream more rapidly than the averaged-velocity profile (Fig. 3a–c). As a result the formation of a nearly quasihomogeneous composition of the mixture over the mixer's cross section is observed even at the distance $x/D \geq 3.1$ (Fig. 6c), which is much earlier than the formation of a uniform averaged-velocity distribution ($x/D > 5.1$) (Fig. 3c). An analysis [5, 26] of the development of the profiles of the averaged mixture fraction and its variance based on the results partially presented in Fig. 6 enables us to state that the recirculation zone begins behind the cross section x/D = 0.1 and degenerates by the cross section $x/X < 5.1$ and its center is located within $2.1 < x/D < 2.6$.

Mixing without a recirculation zone for Q = 5 is slower. As has been shown in [26], the quasiuniform impurity distribution begins to be realized only when x/D = 9.1. The f profile (Fig. 7a–c) expands much more rapidly than the averaged-velocity profile (Fig. 4a–c), which can be due only to the level of intermittency in the shear layer at the jet boundary. The variance profiles of the mixture fraction (Fig. 7d–f) are also wider near their maxima compared to the velocity-pulsation profiles and expand appreciably more rapidly than the latter (Fig. 4d–f). The values of the vari-

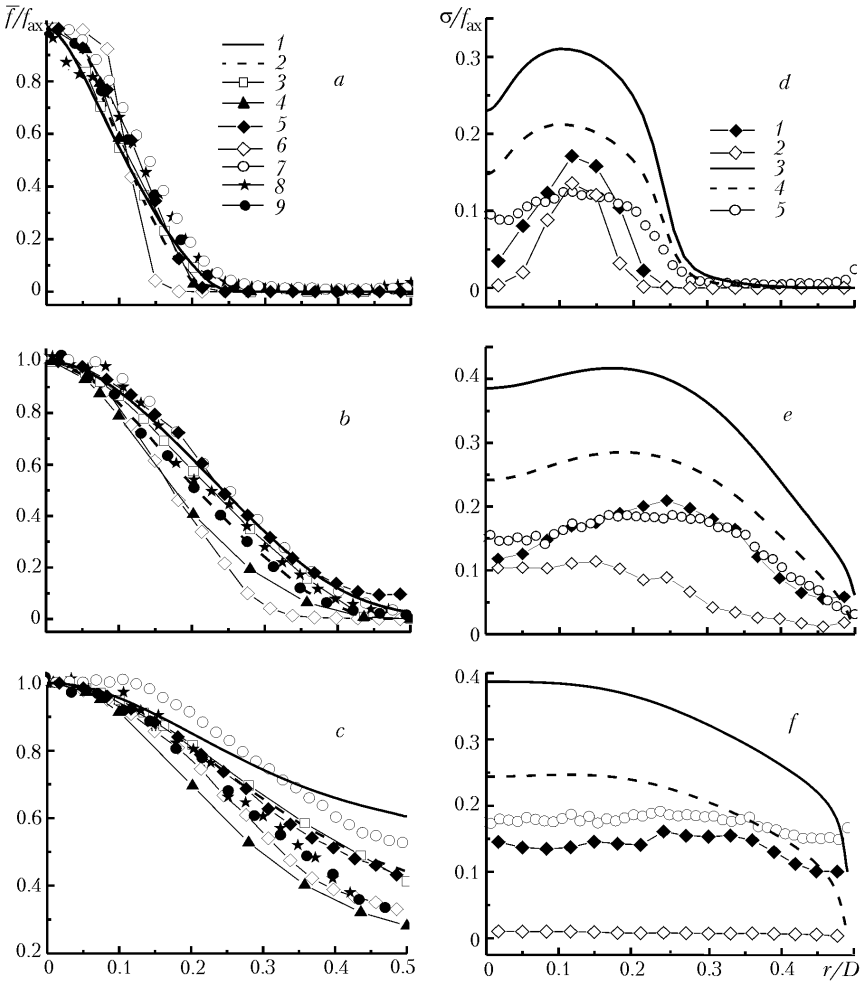

Fig. 7. Averaged mixture fraction $\bar{f}$ (a–c) and its variance σ (d–f) for Q = 5 in the mixer's cross section at different distances from the exit of the jet: a and d) x/D = 1.1, b and e) 3.1, and c and f) 5.1. Notation is the same as in Fig. 6.

ance of the mixture fraction in the region of attainment of macromixing ($x/D \geq 5.1$) are close to the level of velocity pulsations, and in the mixer's cross section x/D = 9.1, they are nearly thrice as large as the values obtained in the mixing regime with a recirculation zone, as has been shown in [26].

Figures 6 and 7 compare the averaged value $f(x, r)$ to the results obtained in [6] using different computational approaches. All the models, except large-eddy simulation with a subgrid Smagorinskii k–ε model with allowance for the dynamic Germano procedure [6], yield identical results compared to experimental data [5]. The difference is in the description of the return-flow region for which the use of the standard k–ε turbulence model (model 5, Table 2) and large-eddy simulation with a subgrid mixed model [6] yields a result more consistent with experiment [5].

Change in the profile of the dispersion σ of the mixture fraction obtained from the two mixing models points to the overstated result in the intensity of scalar pulsations compared to experimental data [5] (Figs. 6 and 7, d–f). Nonetheless, both the large-eddy simulation and the statistical models suggest that the position of local maxima of the profile at the boundary of interaction of the jet and the cocurrent flow for Q = 1.3 (Fig. 6d–f) and for Q = 5 (Fig. 7d–f) is identical to experiment [5].

Analogously to the result on degeneration of the variance of the mixture fraction along the mixer axis (Fig. 5c and d), the cascade mixing model predicts the level of this quantity less adequately than the algebraic mixing model for R = 2. An analysis of the transfer equations for σ^2 in both models enables us to say that the difference is introduced primarily by the approximations of scalar dissipation used. In the algebraic model, the time scale of scalar dissipation is determined by the energy of the developed inertial-convective part of the scalar spectrum, whereas in the

cascade model, it is actually determined by the rate of viscodiffusion mixing determined by the frequency characteristic G which is dependent on the frequency characteristic of micromixing E in small dissipative eddies [23].

Conclusions. The above numerical simulation of mixing in interaction of the turbulent jet and the cocurrent flow of an incompressible fluid (Schmidt number Sc $\approx$ 1000) in the cylindrical channel of a circular cross section (axisymmetric mixer) with the use of different models of calculation of turbulent characteristics enables us to formulate a few basic conclusions.

Two mixing regimes — with a recirculation zone near the channel walls and without it — have been considered for the problem of transfer of a passive impurity in the axisymmetric channel. Such a feature introduces a qualitative difference into the flow structure, which demonstrates that complete mixing takes a shorter period of time in formation of the recirculation zone near the channel walls. This result has been confirmed by an analysis of the degeneration of the calculated longitudinal component of the averaged velocity, kinetic turbulence energy, averaged mixture fraction, and its variance both along the channel axis and over the mixer's cross sections at different distances from the entry of the turbulent jet compared to experiment [5].

The verification of the standard k–ε turbulence model carried out on the basis of experimental data [5] shows that more accurate prediction of the radius of opening and the degeneration of the jet requires modification of the constants in the model equation for kinetic-energy dissipation [25]. The use of different sets of constants known from investigations of free turbulent jets has shown [25] that modification of the constants $C_\mu = 0.06$ and $C_{\varepsilon 2} = 1.87$ in the standard k–ε turbulence model is the best relative to experimental data [5] for the mixing regimes considered. The use of a constant value of the longitudinal velocity instead of the profile in the form of a power law as the boundary condition at exit of the jet points to the existence of a region with a constant velocity to a distance $x/D = 1.5$ for both mixing regimes, which is inconsistent with the change in the longitudinal velocity obtained both experimentally and by large-eddy simulation.

Calculation of the averaged mixture fraction with the use of the standard k–ε model with the values of the constants $C_\mu = 0.06$ and $C_{\varepsilon 2} = 1.87$ and with the velocity profile in the form of a power law at exit of the turbulent jet yields a result analogous to the calculations by the statistical model for Reynolds stresses and by large-eddy simulation for both mixing regimes. However, the mixing models considered (algebraic model for $R = 2$ and the cascade model [23]) yield a result overstated relative to experiment and large-eddy simulation in the change in the variance of the mixture fraction. In the cascade model, the level of pulsations along the mixer axis is nearly 1.5 times higher than the level obtained for the mixing model for $R = 2$ and nearly thrice as high as that in the experiment.

The disagreement revealed point to the need for a more detailed analysis of the capabilities of computational models for predicting turbulent mixing on the basis of the available experimental data.

This work was carried out with support from the Belarusian Republic Foundation for Basic Research (T06MS-042) and the German Scientific-Research Society (DFG).

NOTATION

a, geometric parameter of the mixer; b, density ratio; C, local concentration of the passive impurity; C_0, local concentration of the passive impurity at exit of the turbulent jet; $C_{\sigma 1}$ and $C_{\sigma 2}$, constants of the f–σ^2 model; C_μ, $C_{\varepsilon 1}$, $C_{\varepsilon 2}$, and $C_{\varepsilon 3}$, constants of the k–ε model; D, mixer diameter; D_h, hydraulic diameter; D_{lam}, molecular diffusion coefficient; D_{eff}, effective diffusion coefficient; d, diameter of the mixer's internal tube; E and G, parameters of the cascade f–σ^2 model; F, sought function; f, mixture fraction; f, averaged value of the mixture fraction; f_0, radius-averaged mixture fraction in the mixer's initial cross section; f_{av}, radius-averaged mixture fraction; f_{ax}, averaged value of the mixture fraction on the mixer axis; f_∞, value of the mixture fraction in complete mixing; k, kinetic turbulence energy; l_t, length-scale of turbulence; p, pressure; p_d, exit pressure of the jet; P_ε, extra term in the equation of kinetic-energy dissipation; p_∞, pressure of homogeneous state; Δp_∞, pressure difference; Q, ratio of the flow rates at exit of the turbulent jet and the cocurrent flow; Q_D, flow rate of the cocurrent flow; Q_d, exit flow rate of the jet; Q_∞, flow rate in complete mixing; R, ratio of the characteristic time scales; r, coordinate across the mixer; r_d, radius of opening of the jet; Re_d, Reynolds number calculated from the parameters of the turbulent jet; Re_D, Reynolds number calculated from the parameters of the cocurrent flow; Re_h, Reynolds number calculated from the hydraulic diameter; Re_t, turbulent Reynolds number; S, term responsible for the sources of different nature; Sc, Schmidt number; Sc_t, turbulent Schmidt

number; U, longitudinal component of the averaged velocity; Tu, turbulence intensity; U_{ax}, longitudinal component of the averaged velocity on the mixer axis; U_D and U_d, velocities at entry of the cocurrent flow and at exit of the jet respectively; U_{max}, cross-section-maximum value of the longitudinal velocity (usually on the tube axis); U_∞, velocity in complete mixing; u', standard pulsation of the longitudinal velocity component; V, radial component of the averaged velocity; v', standard pulsation of the radial velocity component; x, coordinate along the mixer; Y, normalized value of f_{av}; α, angular position of the mixer's internal tube; ε, rate of dissipation of the kinetic turbulence energy; ε_s, scalar-dissipation rate; μ_{eff}, effective viscosity; μ_{lam}, molecular dynamic viscosity; μ_t, turbulent viscosity; ρ, density of the mixture; ρ_∞, density of the mixture in complete mixing; σ^2, variance of the mixture fraction; σ_1^2, σ_2^2, and σ_3^2, components of the variance of the mixture fraction; σ_k^2 and σ_ε, turbulent Prandtl numbers; σ_s, integral parameter responsible for the radius of opening of the jet; $\tau_K = \sqrt{(\mu_{lam}/(\rho\varepsilon)}$, Kolmogorov time scale; τ_s, characteristic time scale of scalar mixing; τ_t, characteristic time scale of turbulence. Subscripts: 0, parameter in the mixer's initial cross section; ∞, parameter in complete mixing; av, radius-averaged; ax, axial; D, parameter of the cocurrent flow; d, parameter of the jet; eff, effective; h, hydraulic; lam, laminar; max, maximum; s, parameter of the mixture fraction; t, turbulent.

REFERENCES

1. G. N. Abramovich, *Theory of Turbulent Jets* [in Russian], Izd. Fiz.-Mat. Lit., Moscow (1960).
2. B. A. Kolovandin, *Simulation of Inhomogeneous Turbulence Heat Transfer* [in Russian], Nauka i Tekhnika, Minsk (1980).
3. P. Moin and K. Mahesh, Direct numerical simulation: A tool in turbulence research, *Ann. Rev. Fluid Mech.*, **30**, 539–578 (1998).
4. J. H. Ferziger, Large eddy simulation: its role in turbulence research, in: D. L. Dwoyer, M. Y. Hussaini, and R. G. Voigt (Eds.), *Theoretical Approaches in Turbulence*, Springer-Verlag, New York (1987), pp. 51–72.
5. V. L. Zhdanov, N. V. Kornev, E. Hassel, and A. D. Chorny, Mixing of confined coaxial flows, *Int. J. Heat Mass Transfer*, **49**, 3942–3956 (2006).
6. I. Tkatchenko, N. Kornev, S. Jahnke, G. Steffen, and E. Hassel, Performances of LES and RANS models for simulation of complex flows in a coaxial jet mixer, *Flow, Turbulence and Combustion*, **78**, No. 2, 111–127 (2007).
7. V. L. Zhdanov, N. V. Kornev, and E. Hassel, The influence of the mixer geometry on the scalar field formation, *Lasermethoden in der Strömungsmesstechnik*, 13 Fachtagung, 6–8 September, 2005, Cottbus, Germany (2005), pp. 37-1–37-8.
8. H. J. Henzler, *Investigations on Mixing Fluids*, Doctoral Dissertation, Aachen (1978).
9. H. A. Becker, H. C. Hottel, and G. C. Williams, Mixing and flow in ducted turbulent jets, *Proc. IX Symp. (Int.) on Combustion*, Academic Press, London (1963), pp. 7–20.
10. M. Barchilon and R. Curtet, Some details of the structure of an axis-symmetrical confined jet with backflow, *J. Basic Eng.*, No. 12, 777–787 (1964).
11. A. D. Chornyi and V. L. Zhdanov, Turbulent mixing of a passive admixture in an axisymmetric jet mixer, in: *Proc. 6th Russian National Heat Transfer Conf.*, 19–23 November 2006 [in Russian], Vol. 2, Izd. MÉI, Moscow (2006), pp. 266–269.
12. Yu. V. Lapin and M. Kh. Strelets, *Internal Flows of Gas Mixtures* [in Russian], Nauka, Moscow (1989).
13. S. B. Pope, An explanation of the turbulent round-jet/plane-jet anomaly, *AIAA J.*, **16**, 279–281 (1978).
14. A. Rubel, On the vortex stretching modification of the k–ε-model in radial jets, *AIAA J.*, **23**, 1129–1130 (1985).
15. C. G. Speciale, On nonlinear k–l- and k–ε-models of turbulence, *J. Fluid Mech.*, **178**, 459–475 (1987).
16. B. B. Dally, D. F. Fletcher, and A. R. Masri, Flow and mixing fields of turbulent bluff-body jets and flames, *Combust. Theory Model.*, **2**, 193–219 (1998).
17. F. C. Lockwood and P. Stokalis, Assessment of two turbulence models for turbulent round diffusion jets with combustion, in: *Turbulent Shear Flows*, Vol. 4, Springer-Verlag, Berlin (1983), pp. 328–344.
18. J. J. Mc Guirk and W. Rodi, The calculation of the three-dimensional turbulent free jets, in: F. Durst, B. E. Launder, F. W. Schmidt, and J. H. Whitelaw (Eds.), *Proc. 1st Symp. on Turbulent Shear Flows*, New York (1979), pp. 71–83.

19. J. P. Sanders, B. Sarh, and I. Gokalp, Variable density effects in axisymmetric isothermal turbulent jets: A comparison between a first- and a second-order turbulence model, *Int. J. Heat Mass Transfer*, **40**, No. 4, 823–842 (1997).
20. R. Borghi and D. Escudie, Assessment of a theoretical model of turbulent combustion by comparison with a simple experiment, *Combust. Flame*, **56**, 149–164 (1984).
21. E. J. Smith, G. J. Nathan, and B. B. Dally, Range of validity of a modified k–ε model of the non-reacting flow from a precessing jet nozzle, *Proc. III Int. Conf. on CFD in the Minerals and Process Industries* (CSIRO), 10–12 December 2003, Melbourne, Australia (2003), pp. 499–504.
22. R. Luppes, *The Numerical Simulation of Turbulent Jets and Diffusion Flames*, PhD Thesis, Eindhoven (2000).
23. J. Baldyga and J. R. Bourne, *Turbulent Mixing and Chemical Reactions*, Wiley & Sons, New York (1999).
24. F. E. Kruis and L. Falk, Mixing and reaction in a tubular jet reactor: A comparison of experiments with a model based on a prescribed PDF, *Chem. Eng. Sci.*, **51**, No. 10, 2439–2448 (1996).
25. A. D. Chornyi, Numerical simulation of the interaction of turbulent jets with a co-current flow in a cylindrical channel, *Dokl. Nats. Akad. Nauk Belarusi*, **51**, No. 1, 104–110 (2007).
26. V. L. Zhdanov, A. D. Chornyi, and É. Hassel, Analysis of the process of mixing a passive admixture in a jet mixer, *Inzh.-Fiz. Zh.*, **80**, No. 2, 46–59 (2007).
27. P. J. Guiraud, J. Bertrand, and J. Costes, Laser measurements of local velocity and concentration in a turbulent jet-stirred tubular reactor, *Chem. Eng. Sci.*, **46**, 1289–1297 (1991).